New Closed-Form Green's Functions for Microstrip Structures—Theory and Results

Yuehe Ge, *Student Member, IEEE,* and Karu P. Esselle, *Senior Member, IEEE*

***Abstract*—This paper presents an efficient technique to evaluate the Green's functions of single-layer and multilayer structures. Using the generalized pencil of function method, a Green's function in the spectral domain is accurately approximated by a short series of exponentials, which represent images in spatial domain. New compact closed-form spatial-domain Green's functions are found from these images using several semi-infinite integrals of Bessel functions. With the numerical integration of the Sommerfeld integrals avoided, this method has the advantages of speed and simplicity over numerical techniques, and it leads to closed-form expressions for the method-of-moments matrix coefficients. Numerical examples are given and compared with those from numerical integration.**

***Index Terms*—Complex image method, layered, method of moments, multilayered, Sommerfeld integrals.**

I. Introduction

MICROSTRIP structures are widely used in the hybrid and monolithic microwave integrated circuits (MICs) and microstrip antennas. Numerical modeling of such structures can be efficiently and rigorously performed using the method of moments (MoM). This method requires the computation of Green's functions for layered or multilayered structures, which, in the spatial domain, include oscillatory integrals with infinite limits, i.e., Sommerfeld integrals (SIs).

In modeling microstrip structures using the MoM, much effort has been devoted to the computation of the Green's functions because the computation of SIs are very time consuming. The following three methods can be found in the literature for the evaluation of SIs:

1) numerical integration method;
2) symptotic method;
3) discrete complex image method.

The numerical integration method, described in [1] and [2], is suitable only when the field points are very close to the source points. Generally, this method requires the largest computation time because the integrands are oscillatory. The asymptotic method [3] is the fastest, but it is also the least accurate especially when the field points are close to the source points. They are also complicated and cannot be directly used for multilayer microstrip structures. To address these limitations, a method based on the Sommerfeld identity, called the discrete image method, has been developed [4], [5]. This method first extracts all the quasi-static and surface-wave contributions from the spectral-domain Green's function, and then approximates the remainder by a series of exponentials using the Prony's method [5]. These quasi-static parts, surface-wave parts, and exponentials are interpreted as images with complex displacements, or complex images. By using the Sommerfeld identity, the Sommerfeld integration is done analytically. This discrete image method was improved by Aksun [6], who uses a two-level method and the generalized pencil of function (GPOF) method [7] to approximate the spectral domain without extracting the quasi-static and surface-wave contributions. This method's accuracy depends on the accuracy of the approximation by the series of exponentials, and the GPOF method [7] was found to be very accurate for this purpose. The only previous complex image method that gives closed-form derivatives of the Green's functions is due to [8].

In this paper, we present a new complex image method based on a class of semi-infinite integrals of Bessel functions. Our method can be applied to evaluate both the Green's functions and their derivatives and gives accurate results efficiently. New closed-form expressions for the Green's functions, and their derivatives, can be obtained using this method. When this method is used in conjunction with the MoM, one can derive closed-form expressions for the MoM matrix elements directly. Unlike previous complex image methods, this method does not require a second Taylor-series approximation for this purpose.

II. Spatial-Domain Green's Functions of Multilayer Structures

Consider a current source in a multilayer medium shown in Fig. 1. The source can be x-, y-, or z-directed. Each layer can have different electric and magnetic properties (ε_i, μ_i) and thickness (h_i). The field point can be located in an arbitrary layer. The electric field due to the current can be expressed in a mixed potential form as

$$\mathbf{E} = -\mathbf{j}\omega\mu_0\langle \mathbf{G^A}, \mathbf{J}\rangle + \frac{1}{\mathbf{j}\omega\varepsilon_0}\nabla\langle \mathbf{G^q}, \nabla'\cdot\mathbf{J}\rangle \qquad (1)$$

where $\mathbf{J}$ denotes the electric current density of the source and $\mathbf{G^A}$ and G^q are the spatial-domain Green's functions associated with the vector and scalar potentials, respectively. The details on

Manuscript received April 4, 2000; revised June 12, 2001. This work was supported by the Australian Research Council, by the Macquarie University International Postgraduate Research Scholarship Scheme, and by the 2000 IEEE Microwave Theory and Techniques Society (IEEE MTT-S) under a graduate fellowship award.

The authors are with the Department of Electronics, Division of Information and Communication Sciences, Macquarie University, Sydney, N.S.W. 2109, Australia (e-mail: yuehe@ics.mq.edu.au; esselle@elec.mq.edu.au).

Publisher Item Identifier S 0018-9480(02)05218-3.

0018-9480/02$17.00 © 2002 IEEE

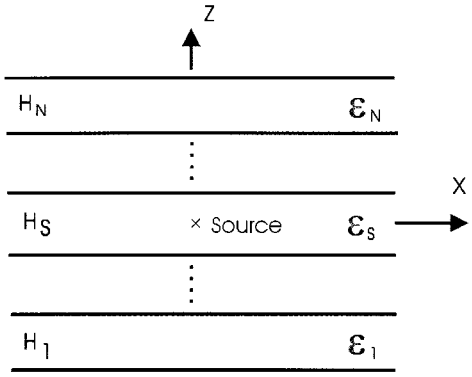

Fig. 1. Multilayer planar structure.

$\mathbf{G^A}$ for a horizontal source have been discussed in [9], [10], and [11], and one may represent it as

$$\mathbf{G^A} = \begin{bmatrix} \mathbf{G^A_{xx}} & 0 & \mathbf{G^A_{xz}} \\ 0 & \mathbf{G^A_{yy}} & \mathbf{G^A_{yz}} \\ \mathbf{G^A_{zx}} & \mathbf{G^A_{zy}} & \mathbf{G^A_{zz}} \end{bmatrix}. \tag{2}$$

All of the above various forms of spatial-domain Green's functions ($\mathbf{G^A_{ij}}, G^q$) and their derivatives can be represented in the following shorthand form:

$$S_n[f] = \int_C H_n^{(2)}(k_\rho\rho) k_\rho^{n+1} f(k_\rho)\, dk_\rho, \qquad n = 0, 1 \tag{3}$$

where $H_n^{(2)}$ is the Hankel function of the second kind and nth order, ρ is the radial distance in the x-y-plane between the field points and source points, k_ρ is the radial propagation constant in the x-y-plane, and C is the integration path. The function $f(k_\rho)$ is the spectral-domain Green's function, which can be obtained analytically for a multilayer medium.

In practical applications, $n = 1$ type integrals arise when the derivatives of Green's functions are involved. In the MoM, often the derivatives of the Green's functions can be combined with the basis and testing functions and then, by using the integration by parts, they can be converted to $n = 0$ type integrals. However, there exist some cases in which this conversion is not possible and then one has to integrate $n = 1$ type integrals.

III. New Complex Image Method

A. Theory

By using the integral relationship, we rewrite integral (3) as [1]

$$\int_C H_n^{(2)}(k_\rho\rho) k_\rho^{n+1} f(k_\rho)\, dk_\rho = 2\int_0^\infty J_n(k_\rho\rho) k_\rho^{n+1} f(k_\rho)\, dk_\rho \tag{4}$$

where J_n is the Bessel function of the first kind and nth order.

The SIs like (3) and (4) cannot be evaluated analytically. In previous complex image methods, the spectral-domain Green's function $f(k_\rho)$ was approximated by a series of complex exponentials as

$$f(k_\rho) = \frac{1}{jk_z} \sum_{i=1}^{M} \alpha_i e^{-\beta_i k_z} \tag{5}$$

where $k_z = \sqrt{k_0^2 - k_\rho^2}$, k_0 is the propagation constant in free space, and α_i and β_i were unknown coefficients to be determined using an approximation technique. The Sommerfeld identity was then used to obtain a closed-form solution for the integral in (3) as follows:

$$\int_0^\infty \frac{e^{-jk_z|z|}}{jk_z} J_0(k_\rho\rho) k_\rho\, dk_\rho = \frac{e^{-jk_0 r}}{r} \tag{6}$$

where $r = \sqrt{\rho^2 + z^2}$. By substituting approximation (5) into (4) and using (6), one obtains

$$S_0[f] = 2\sum_{i=1}^{M} \alpha_i \frac{e^{-jk_0 r}}{r} \tag{7}$$

where $r = \sqrt{\rho^2 - \beta_i^2}$. Details of this method can be found in [5]. Although $S_1[f]$ can be obtained from the derivative of (7) [8], this method cannot be used directly to derive closed-form expressions for the MoM matrix elements.

In this paper, we use a different series expansion. Using a class of semi-infinite integrals of Bessel functions, we then derive the closed-form solutions of SIs $S_n[f]$ for both the $n = 0$ and $n = 1$ cases. The resulting expressions are simpler than those from previous methods and they can be used directly in conjunction with the MoM. Suppose we can approximate the function $f(k_\rho)$ by a sum of complex exponentials

$$k_\rho^{n+1} f(k_\rho) \cong k_\rho \sum_{i=1}^{M} a_i e^{-b_i k_\rho} \tag{8}$$

where a_i, b_i are the unknown coefficients and exponents. They are obtained by the application of an approximation technique, such as the GPOF method, as explained in Section III-B. Rewriting (4), we have

$$\int_C H_n^{(2)}(k_\rho\rho) k_\rho^{n+1} f(k_\rho)\, dk_\rho = 2\sum_{i=1}^{M} a_i \int_0^\infty J_n(k_\rho\rho) k_\rho e^{-b_i k_\rho}\, dk_\rho. \tag{9}$$

The right-hand side of (9) is a semi-infinite integral of Bessel functions, which can be solved analytically using the following semi-infinite integrals of Bessel functions:

$$\int_0^\infty e^{-k_\rho w} k_\rho J_0(k_\rho\rho)\, dk_\rho = \frac{w}{(w^2 + \rho^2)^{(3/2)}} \tag{10}$$

$$\int_0^\infty e^{-k_\rho w} k_\rho J_1(k_\rho\rho)\, dk_\rho = \frac{\rho}{(w^2 + \rho^2)^{(3/2)}}. \tag{11}$$

After the analytical integration, one obtains the following closed-form expressions for $S_n[f]$:

$$S_0[f] = 2\sum_{i=1}^{M} \frac{a_i b_i}{(b_i^2 + \rho^2)^{(3/2)}} \tag{12}$$

$$S_1[f] = 2\sum_{i=1}^{M} \frac{a_i \rho}{(b_i^2 + \rho^2)^{(3/2)}}. \tag{13}$$

Generally, the use of Bessel integrals (10) and (11) leads to good results. However, there are other Bessel integrals that may also

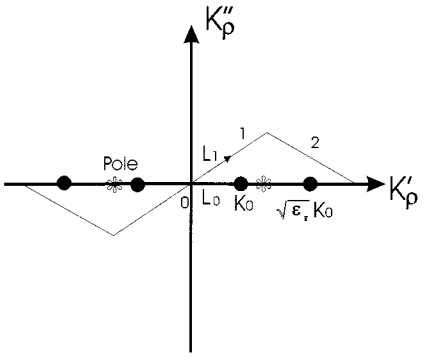

Fig. 2. Integration contours L_0 and L_1 on the complex k_ρ-plane.

be used in this method. Four such alternative integrals of Bessel functions are given in the Appendix. Each choice leads to a different closed-form Green's function.

The use of the two closed-form Green's functions (12) and (13) in conjunction with the MoM gives rise to closed-form expressions for MoM matrix elements. Hence, a significant improvement in the matrix-fill time can be achieved.

B. Two-Level Approximation of the Spectral-Domain Green's Functions

The accuracy of this method in general depends on the accuracy of the approximation of spectral-domain Green's functions using complex exponentials.

In this section, we will discuss how we approximated the spectral-domain Green's functions. We have selected an integration path suitable for (10) and (11) and used a two-level approximation technique [6] to perform the approximation in a robust fashion. It should be noted that the complex images in our method are distributed on the complex k_ρ-plane, while the images obtained in the previous method [5], [6] are on the complex k_z-plane. We then used (10) and (11) to complete the integration. We selected the integration path shown as L_1 in Fig. 2, which is different from the arc and line path used in previous methods [6].

The integration can be performed along the real axis L_0 on the complex k_ρ-plane or along a deformed path L_1 passing through the origin and lying in the first and third quadrants, as shown in Fig. 2. The integration path L_0 can be deformed to L_1 since no singularity is encountered in the deformation. Since the function $f(k_\rho)$ is close to zero when the k_ρ is large enough, we choose a finite integration path L_1, which is composed of two straight lines.

The parametric equations of the two straight lines are

$$\begin{aligned} L_1^1&: k_\rho = t + j\frac{t}{T_0}, \qquad 0 \le t \le t_0 \\ L_1^2&: k_\rho = t + j\frac{(t_1 - t)t_0}{T_0(t_1 - t_0)}, \qquad t_0 \le t \le t_1 \end{aligned} \tag{14}$$

where t_0 and t_1 are the two values on the real axis of the complex k_ρ-plane corresponding to the ends of the two straight lines (1 and 2 in Fig. 2) and T_0 is the gradient of the straight line 1. By selecting suitable values for the parameters t_0, t_1, and T_0, good results can be obtained.

For the approximation, the GPOF method [7] is a good choice because we do not need to consider the quasi-static images and surface-wave poles (SWPs) when performing the approximation of the spectral-domain Green's functions. However, for some reasons, which have been discussed in [6], it is difficult to make the approximation in $[0, t_1]$ properly. One of the reasons is that the proper t_1 may be very large, and we need a large number of samples to perform the approximation, which is not a robust approach. After investigating the spectral-domain Green's functions, we decided to use a two-level approximation, as explained below. The first part of the approximation is performed along the path L_1^1, while the second part is done along the path L_1^2. Generally, the Green's functions change rapidly in the first part $[0, t_0]$, while decay smoothly in the second part $[t_0, t_1]$; thus, we choose more samples and exponentials to perform the approximation in the first part.

The main steps of the two-level approximation are outlined as follows.

Step 1) Choose t_0 and t_1 such that $t_0 < t_1$ and $f(t_1) < \varepsilon$, where ε is a number small enough such that we can ignore values smaller than ε (typically, $\varepsilon \approx 10^{-4}$).

Step 2) Choose T_0 and the number of samples on $[t_0, t_1]$. The choice of T_0 is very critical, and it determines the precision of the approximation.

Step 3) Sample the function $f(k_\rho)$ along the path L_1^2 and approximate it by using the GPOF method so that

$$f(k_\rho) \cong F_2 = \sum_{j=1}^{M_2} a_j e^{-b_j k_\rho}, \qquad \text{on } [t_0, t_1].$$

Step 4) Subtract F_2 from the original function $f(k_\rho)$ on $[0, t_0]$. (We ignore the difference $f(k_\rho) - F_2$ when $k_\rho > t_0$, i.e., on $[t_0, t_1]$.)

Step 5) Sample the function $f(k_\rho) - F_2$ uniformly along the path L_1^1 and approximate it by using the GPOF method as follows:

$$f(k_\rho) - F_2 = F_1 = \sum_{i=1}^{M_1} c_i e^{-d_i k_\rho}, \qquad \text{on } [0, t_0].$$

After the above steps, we obtain

$$\begin{aligned} S_0[f] &= \int_{L_1^1} H_0^{(2)}(k_\rho \rho) k_\rho F_1 \, dk_\rho \\ &\quad + \int_{L_1^1 + L_1^2} H_0^{(2)}(k_\rho \rho) k_\rho F_2 \, dk_\rho \\ &\approx \sum_{i=1}^{M_1} \frac{c_i d_i}{(d_i^2 + \rho^2)^{1.5}} + \sum_{j=1}^{M_2} \frac{a_j b_j}{\left(b_j^2 + \rho^2\right)^{1.5}} \end{aligned} \tag{15}$$

and the same procedure is followed for $S_1[f]$ when $n = 1$.

In one of the previous complex image methods, all the quasi-static images [5] and SWPs [2], [5] were extracted from the spectral-domain Green's function $f(k_\rho)$ and then the remainder was approximated by a series of complex exponentials using the Prony's method [5]. It is true that the approximation using the Prony's method gives accurate results with the extraction of the quasi-static images and SWP. However, there is no general method to find the quasi-static images of the Green's functions

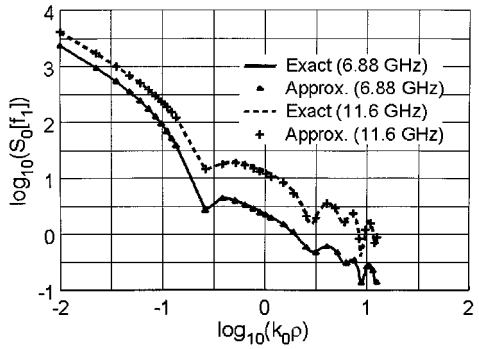

Fig. 3. Amplitude of the SI $S_0[f_1]$ for two cases. (a) Frequency $= 6.88$ GHz. Substrate height $(\mathrm{h}) = 0.64$ mm, $\varepsilon_r = 10.2$. (b) Frequency $= 11.6$ GHz. Substrate height $(\mathrm{h}) = 0.64$ mm, $\varepsilon_r = 10.2$.

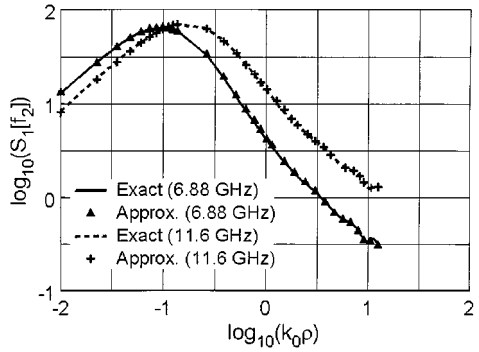

Fig. 4. Amplitude of the SI $S_1[f_2]$ for two cases. (a) Frequency $= 6.88$ GHz. Substrate height $(\mathrm{h}) = 0.64$ mm, $\varepsilon_r = 10.2$. (b) Frequency $= 11.6$ GHz. Substrate height $(\mathrm{h}) = 0.64$ mm, $\varepsilon_r = 10.2$.

of multilayer structures. We have avoided this problem by using the GPOF method. We have found that GPOF method gives accurate results even without the extraction of quasi-static images and SWP. For example, the results in Figs. 3 and 4 were generated without such extraction.

IV. Results

The technique presented here can be used to evaluate the spatial-domain Green's functions for multilayer geometries having an arbitrary number of layers with arbitrary parameters and general (electric or magnetic, horizontal or vertical) sources. To verify the accuracy of our extended complex images method, two numerical examples for single-layer structures are presented in this section and our results are compared with the almost exact results obtained from the numerical integration. One of the examples is the $S_0[f]$ $(n = 0)$ type, and it is related to the G^q. The second is the $S_1[f]$ $(n = 1)$ type, which is related to the derivative of the G^A_{xz}. The example functions are the spectral-domain Green's functions associated with single-layer microstrip structures, given by [1], [2]

$$\mathbf{f_1} = \frac{\mathbf{N_H}}{\mathbf{D_H D_E}} \tag{16}$$

$$\mathbf{f_2} = \frac{1}{\mathbf{D_H D_E}\cosh(\mathbf{u_1 h})} \tag{17}$$

TABLE I
Parameters for Approximation by the GPOF

	t_0	t_1	T_0	N_1	N_2	M_1	M_2
$S_0[f_1]$	$2k_1$	$10k_1$	10	50	30	9	7
$S_1[f_2]$	$2.2k_1$	$7k_1$	10	50	30	9	7

where

$$\mathbf{D_H} = \mathbf{u_0} + \mathbf{u_1}\coth(\mathbf{u_1 h})$$
$$\mathbf{D_E} = \varepsilon_\mathbf{r}\mathbf{u_0} + \mathbf{u_1}\tanh(\mathbf{u_1 h})$$
$$\mathbf{N_H} = \mathbf{u_0} + \mathbf{u_1}\tanh(\mathbf{u_1 h})$$
$$\mathbf{u_0} = \sqrt{\mathbf{k_\rho^2} - \mathbf{k_0^2}}$$
$$\mathbf{u_1} = \sqrt{\mathbf{k_\rho^2} - \varepsilon_\mathbf{r}\mathbf{k_0^2}}.$$

These two examples are evaluated using two different sets of parameters. Table I lists the t_0, t_1, and T_0 we choose for these calculations.

In Table I, $k_1 = \sqrt{\varepsilon_r}k_0, N_1$ and N_2 are the number of samples in the first and second parts of the approximation, respectively, and M_1 and M_2 are the number of exponentials used in the first and second parts of the approximation, respectively.

Figs. 3 and 4 show the amplitudes of the two SIs computed by the approximate method in this paper and by the numerical integration (almost exact). It can be seen that the results from the two methods compare very well. It should be noted that each numerical integration takes more than 1 min in a typical workstation, but the new method gives results in a fraction of a second.

V. Conclusion

We have presented a new more flexible complex image method based on a class of semi-infinite integrals of Bessel functions, for the evaluation of SIs encountered in Green's functions, and their derivatives of layered structures. Through the use of a two-level approximation of the spectral-domain Green's functions, closed-form expressions have been derived for the SIs. This method can handle both $n = 0$ and $n = 1$ type SIs. The resulting closed-form solutions can be directly used in the MoM without additional approximations. It is significantly faster than the numerical integration method, but it gives accurate results. Numerical examples of the new closed-form Green's functions have been presented. The results are compared with accurate results from the numerical integration method and a very good agreement is observed.

Appendix

Alternative integrals for the $n = 0$ case, i.e., $S_0[f]$, are as follows:

$$\int_0^\infty e^{-k_\rho w} J_0(k_\rho\rho)\, dk_\rho = \frac{1}{\sqrt{w^2+\rho^2}} \tag{A1}$$

$$\int_0^\infty e^{-k_\rho w} k_\rho^2 J_0(k_\rho\rho)\, dk_\rho = \frac{2w^2-\rho^2}{(w^2+\rho^2)^{(5/2)}}. \tag{A2}$$

Alternative integrals for the $n = 1$ case, i.e., $S_1[f]$, are as follows:

$$\int_0^\infty e^{-k_\rho w} J_1(k_\rho \rho)\, dk_\rho = \frac{1}{\rho}\left(1 - \frac{w}{\sqrt{w^2+\rho^2}}\right) \quad \text{(A3)}$$

$$\int_0^\infty e^{-k_\rho w} k_\rho^2 J_1(k_\rho \rho)\, dk_\rho = \frac{3\rho w}{(w^2+\rho^2)^{(5/2)}}. \quad \text{(A4)}$$

REFERENCES

[1] J. R. Mosig and F. E. Gardiol, "A dynamical radiation model for microstrip structures," *Adv. Electron. Electron Phys.*, vol. 59, pp. 139–237, 1982.

[2] J. R. Mosig and T. K. Sarkar, "Comparison of quasi-static and exact electromagnetic fields from a horizontal electric dipole above a lossy dielectric backed by an imperfect ground plane," *IEEE Trans. Microwave Theory Tech.*, vol. MTT-34, pp. 379–387, Apr. 1986.

[3] S. Barkeshli, P. H. Pathak, and M. Marin, "An asymptotic closed-form microstrip surface Green's function for the efficient moment method analysis of mutual coupling in microstrip antenna," *IEEE Trans. Antennas Propagat.*, vol. 38, pp. 1374–1383, Sept. 1990.

[4] D. G. Fang, J. J. Yang, and G. Y. Delisle, "Discrete image theory for horizontal electric dipoles in a multilayered medium," in *Proc. Inst. Elect. Eng.*, vol. 135, Oct. 1988, pp. 297–303.

[5] Y. L. Chow, J. J. Yang, D. G. Fang, and G. E. Howard, "A closed-form spatial Green's function for the thick microstrip substrate," *IEEE Trans. Microwave Theory Tech.*, vol. 39, pp. 588–592, Mar. 1991.

[6] M. I. Aksun, "A robust approach for the derivation of closed-form Green's functions," *IEEE Trans. Microwave Theory Tech.*, vol. 44, pp. 651–658, May 1996.

[7] Y. Hua and T. K. Sarkar, "Generalized pencil-of-function method for extracting poles of an EM system from its transient response," *IEEE Trans. Antennas Propagat.*, vol. 37, pp. 229–234, Feb. 1989.

[8] N. Hojjat, S. Safavi-Naeini, R. Faraji-Dana, and Y. L. Chow, "Fast computation of the nonsymmetrical components of the Green's function for multilayer media using complex images," in *Proc. Inst. Elect. Eng.*, vol. 145, Aug. 1998, pp. 285–288.

[9] W. C. Chew, *Waves and Fields in Inhomogeneous Media*. New York: Van Nostrand, 1990.

[10] K. A. Michalski and D. Zheng, "Electromagnetic scattering and radiation by surfaces of arbitrary shape in layered media—Part I: Theory," *IEEE Trans. Antennas Propagat.*, vol. 38, pp. 335–344, Mar. 1990.

[11] K. A. Michalski and J. R. Mosig, "Multilayered media Green's functions in integral equation formulations," *IEEE Trans. Antennas Propagat.*, vol. 45, pp. 508–519, Mar. 1997.

Yuehe Ge (S'99) received the B.S. and M.S. degrees in radio engineering from the Nanjing University of Posts and Telecommunications, Nanjing, China, in 1988 and 1991, respectively, and is currently working toward the Ph.D. degree in electronics at Macquarie University, Sydney, N.S.W., Australia.

From 1991 to 1999, he was with the Nanjing Marine Radar Institute, Nanjing, China, where he was involved with the research and development of radar antennas and microwave components. His current research interests involve numerical methods for electromagnetics and antenna development for radar and communication applications.

Mr. Ge was a recipient of the 2000 IEEE Microwave Theory and Techniques Society (IEEE MTT-S) Graduate Fellowship Award.

Karu P. Esselle (M'92–SM'96) received the B.Sc. degree in electronic and telecommunication engineering (with first-class honors) from the University of Moratuwa, Moratuwa, Sri Lanka, in 1983, and the M.A.Sc. and Ph.D. degrees in electrical engineering from the University of Ottawa, Ottawa, ON, Canada, in 1987 and 1990, respectively.

From 1984 to 1985, he was an Assistant Lecturer with the University of Moratuwa. From 1987 to 1990, he was a Research Assistant with the University of Ottawa. From 1990 to 1992, he was a Canadian Government Laboratory Visiting Post-Doctoral Fellow. In 1992, he joined Macquarie University, Sydney, N.S.W., Australia, where he is currently a Senior Lecturer of electronics. From 1996 to 1997, he was a Visiting Professor with the University of Victoria, Victoria, BC, Canada. His industrial experience includes full-time positions as a Faculty Hire Design Expert of the Hewlett-Packard Laboratory, Palo Alto, CA, in 1996, and several consultancies from 2000 to 2001. He has authored or co-authored over 70 papers. His research has been sponsored by many organizations including the Australian Research Council, the Department of Industry, Science, and Tourism, and Macquarie University (Research Fellowship scheme). His current research interests include antennas for wireless communication systems including 5-GHz wireless computer networks, dielectric resonator (DR) antennas, microstrip antennas, printed inverse F antennas (PIFAs), hybrid dielectric and patch antennas, finite-difference time-domain (FDTD) methods for thin metal films and strips, FDTD methods for high-speed digital circuits, moment methods for DRs, hybrid, microstrip, and slot antennas, complex image methods and closed-form Green's functions for layered structures, Luneberg and other lens antennas for radio telescopes, and photonic-bandgap structures for antenna and microwave applications.

Dr. Esselle was an organizer and the publicity chair of the 2000 Asia–Pacific Microwave Conference. He has been the chair of the IEEE New South Wales Microwave Theory and Techniques Society (MTT-S)/Antennas and Propagation Society (AP-S) Joint Chapter since 1999. He was the recipient of a Canadian Commonwealth Scholarship (1985–1990). He was the recipient of the 1990 Young Scientist Award of the International Scientific Radio Union (URSI).